Elimination of fast variables in stochastic nonlinear kinetics

Gabriel Morgado[1,2], Bogdan Nowakowski[1,3], and Annie Lemarchand[2]

[1]Institute of Physical Chemistry, Polish Academy of Sciences, Kasprzaka 44/52, 01-224 Warsaw, Poland
[2]Laboratoire de Physique Théorique de la Matière Condensée, Sorbonne Université, CNRS , 4 place Jussieu, case courrier 121, 75252 Paris CEDEX 05, France
[3]SGGW, Warsaw University of Life Sciences, Nowoursynowska 159, 02-776 Warsaw, Poland

Abstract

A reduced chemical scheme involving a small number of variables is often sufficient to account for the deterministic evolution of the concentrations of the main species contributing to a reaction. However its predictions are questionable in small systems used for example in fluorescence correlation spectroscopy (FCS) or in explosive systems involving strong nonlinearities such as autocatalytic steps. We make precise dynamical criteria defining the validity domain of the quasi-steady-state approximation and the elimination of a fast concentration in deterministic dynamics. Designing two different three-variable models converging toward the same two-variable model, we show that the variances and covariance of the fluctuations of the slow variables are not correctly predicted by the two-variable model, even in the limit of a large system size. The more striking weaknesses of the reduced scheme are figured out in mesoscaled systems containing a small number of molecules. The results of two stochastic approaches are compared and the shortcomings of the Langevin equations with respect to the master equation are pointed out. We conclude that the description of the fluctuations and their coupling with nonlinearities of deterministic dynamics escape reduced chemical schemes.

1   Introduction

The quasi-steady-state approximation is currently used in chemistry to eliminate a fast vari-

able and build tractable reaction mechanisms involving a few species while satisfactorily

accounting for the dynamical behavior of the system [1, 2, 3, 4]. However, in a small system, containing a small number of particles, fluctuations reach large amplitudes [5]. Our goal is to make precise how eliminating a fast variable in a model of growing Turing pattern [6] may affect the prediction on the amplitude of concentration fluctuations. The interplay between nonlinearities of deterministic dynamics and fluctuations makes the elimination of fast variables in stochastic dynamics non trivial [7, 8, 9, 10, 11, 12]. The issue is essential to estimate the ability of a reduced chemical scheme to report on experiments in small samples such as fluorescence correlation spectroscopy (FCS) experiments [13, 14]. To this purpose we consider a minimal chemical model involving two species of variable concentrations, able to reproduce the propagation of a chemical wave front toward a stable steady state and a spatially-periodic structure of Turing type [15, 16, 17, 18]. The minimum model is assumed to result from the reduction of three-variable models. The question is to determine if the amplitude of the fluctuations deduced from a three-variable model is correctly predicted by the two-variable model, in the limit where the reduction of deterministic dynamics is valid and for homogeneous conditions in the vicinity of a steady state.

The paper is organized as follows. In section 2, we determine the conditions on the parameters for the deterministic dynamics of the two- and three-variable models to be as close as possible. In particular, we look for conditions ensuring that the steady states coincide in order to make the comparison between the models relevant. Section 3 is devoted to the stochastic description of the different models. Langevin equations with internal noise [19] deduced from the chemical master equation are used to derive analytical expressions of the variances and covariances of concentration fluctuations for the two-variable and three-variable models [20, 21, 22]. Choosing the nontrivial stable steady state of the two-variable and three-variable models as initial condition, we simulate the master equation using the kinetic Monte Carlo method introduced by Gillespie [23] and determine the variances and covariance of the fluctuations of the slow variables. The accuracy of the Langevin approach is checked

by comparing the results given by the two stochastic approaches. Section 4 is devoted to discussion and conclusion.

2 Deterministic dynamics

2.1 The two-variable model

The following chemical mechanism, inspired by the Schnakenberg model [24] and the Gray-Scott model [25], has been designed to account for different self-organization phenomena in open systems [26]

$$X \xrightarrow{k_1} R_1 \tag{1}$$

$$2\,X + Y \xrightarrow{k_2} 3\,X \tag{2}$$

$$Y \xrightleftharpoons[k'_{-3}]{k_3} R_2 \tag{3}$$

In particular, we used it to study the impact of fluctuations [15] on growing Turing structures with possible application to the development of periodic patterns in embryos [16, 17, 18]. The concentrations of the species R_1 and R_2 are assumed to be constant through appropriate matter exchanges with reservoirs, also called chemostats by analogy with thermostats capable of fixing temperature through heat exchanges. The model involves two species X and Y of variable concentrations X and Y governed by the following differential equations

$$\frac{\mathrm{d}X}{\mathrm{d}t} = -k_1 X + k_2 X^2 Y \tag{4}$$

$$\frac{\mathrm{d}Y}{\mathrm{d}t} = k_{-3} - k_3 Y - k_2 X^2 Y \tag{5}$$

where the k_i's, for $i = 1, 2, 3, -3$, are rate constants. For the sake of simplicity, we set $k_{-3} = k'_{-3} R_2$.

For parameter values obeying $\Delta < 0$ with $\Delta = k^2_{-3} - 4k_1^2 k_3/k_2$, the two-variable model admits a single steady state $(X_2^0 = 0, Y_2^0 = k_{-3}/k_3)$. If $\Delta \geq 0$, the model has three stationary

states (X_2^0, Y_2^0), (X_1^0, Y_1^0), and (X_0^0, Y_0^0) with

$$X_1^0 = \frac{k_{-3} - \sqrt{\Delta}}{2k_1} \tag{6}$$

$$Y_1^0 = \frac{k_{-3} + \sqrt{\Delta}}{2k_3} \tag{7}$$

$$X_0^0 = \frac{k_{-3} + \sqrt{\Delta}}{2k_1} \tag{8}$$

$$Y_0^0 = \frac{k_{-3} - \sqrt{\Delta}}{2k_3} \tag{9}$$

In the domain of existence of the three stationary states, (X_1^0, Y_1^0) is unstable whereas (X_0^0, Y_0^0) and (X_2^0, Y_2^0) are stable. The model has been designed to have a steady state obeying $X_2^0 = 0$, unable to create X species *ex nihilo* and consequently insensitive to internal fluctuations. Hence, in a spatially extended system, it is possible to prepare a region of space in the state (X_2^0, Y_2^0) and study how it is invaded by a propagating chemical wave front. After the passage of the wave front, the system relaxes towards the steady state (X_0^0, Y_0^0) and can be destabilized by inhomogeneous perturbations, being then replaced by a periodic spatial pattern of Turing type [16, 17, 18].

In the following, we focus on a homogeneous system and study the linear dynamics in the vicinity of the steady state (X_0^0, Y_0^0). Introducing the deviations $x = X - X_0^0$ and $y = Y - Y_0^0$ from the steady state, we locally characterize dynamics by the linearized equations

$$\frac{d\zeta}{dt} = \mathbf{M}\zeta \tag{10}$$

where $\zeta = \begin{pmatrix} x \\ y \end{pmatrix}$ is the vector representing the deviation from the steady state and $\mathbf{M}$ is the stability matrix, given by

$$\mathbf{M} = \begin{pmatrix} m_{11} = k_1 & m_{12} = k_2(X_0^0)^2 \\ m_{21} = -2k_1 & m_{22} = -k_3 - k_2(X_0^0)^2 \end{pmatrix} \tag{11}$$

The eigenvalues of $\mathbf{M}$ are

$$\lambda_1^0 = \frac{k_1 - k_3 - k_2(X_0^0)^2 + \sqrt{\Delta'}}{2} \tag{12}$$

$$\lambda_2^0 = \frac{k_1 - k_3 - k_2(X_0^0)^2 - \sqrt{\Delta'}}{2} \tag{13}$$

with $\Delta' = (k_2(X_0^0)^2 + k_3 - k_1)^2 - 4k_1(k_2(X_0^0)^2 - k_3)$ and X_0^0 given in Eq. (8). The vector $\chi = \begin{pmatrix} x_1 \\ x_2 \end{pmatrix}$ of coordinates in the eigenbasis of $\mathbf{M}$ is related to the vector ζ through $\zeta = \mathbf{P}^0\chi$ where the change of basis matrix is

$$\mathbf{P}^0 = \begin{pmatrix} p_{11}^0 = k_2(X_0^0)^2 & p_{12}^0 = k_2(X_0^0)^2 \\ p_{21}^0 = \lambda_1 - k_1 & p_{22}^0 = \lambda_2 - k_1 \end{pmatrix} \tag{14}$$

The dynamics around the steady state is locally characterized by the two relaxation times $\tau_i^0 = 1/\mid R(\lambda_i^0) \mid$, with $i = 1, 2$, where R returns the real part of the argument.

Two different three-variable models converging to the two-variable model after elimination of a fast variable Z are introduced in the next subsections.

2.2 Three-variable model A

One of the simplest way to introduce a third variable concentration Z consists in considering an intermediate species Z [27], reversibly formed through the second reaction with rate constants k_2' and k_{-2}' and irreversibly transformed into 3X with rate constant k_2'' according to the three-variable model A

$$X \xrightarrow{k_1} R_1 \tag{15}$$

$$2\,X + Y \underset{k_{-2}'}{\overset{k_2'}{\rightleftarrows}} Z \tag{16}$$

$$Z \xrightarrow{k_2''} 3\,X \tag{17}$$

$$Y \underset{k_{-3}}{\overset{k_3}{\rightleftarrows}} R_2 \tag{18}$$

The goal of this subsection is to determine the conditions for which the three-variable model reduces to the two-variable model. The rate equations associated with model A are

$$\frac{\mathrm{d}X}{\mathrm{d}t} = -k_1 X - 2k_2' X^2 Y + (2k_{-2}' + 3k_2'')Z \tag{19}$$

$$\frac{\mathrm{d}Y}{\mathrm{d}t} = k_{-3} - k_3 Y - k_2' X^2 Y + k_{-2}' Z \tag{20}$$

$$\frac{\mathrm{d}Z}{\mathrm{d}t} = k_2' X^2 Y - (k_{-2}' + k_2'')Z \tag{21}$$

On the slow manifold [28, 29, 4] defined by $\frac{\mathrm{d}Z}{\mathrm{d}t} = 0$, i.e.

$$Z = \frac{k_2'}{k_{-2}' + k_2''} X^2 Y \tag{22}$$

5

dynamics becomes

$$\frac{\mathrm{d}X}{\mathrm{d}t} = -k_1 X + \frac{k_2' k_2''}{k_{-2}' + k_2''} X^2 Y \tag{23}$$

$$\frac{\mathrm{d}Y}{\mathrm{d}t} = k_{-3} - k_3 Y - \frac{k_2' k_2''}{k_{-2}' + k_2''} X^2 Y \tag{24}$$

which exactly matches the dynamics of the two-variable model given in Eqs. (4,5) provided that:

$$\frac{k_2' k_2''}{k_{-2}' + k_2''} = k_2 \tag{25}$$

In particular, when the above condition is satisfied, the steady state (X_0, Y_0, Z_0) of model A obeys

$$X_0 = X_0^0 \tag{26}$$

$$Y_0 = Y_0^0 \tag{27}$$

$$Z_0 = \frac{k_1 X_0^0}{k_2''} \tag{28}$$

where the expression of the steady concentrations X_0^0 and Y_0^0 for the two-variable model are given in Eqs. (8,9). Provided that Eq. (25) is obeyed, the steady concentrations of the three-variable model A do not depend on the rate constants k_2' and k_{-2}'. The variation of the steady concentrations versus the rate constant k_2'' is given in Fig. 1 for the two-variable model and the three-variable model A. For the chosen parameter values, the steady concentration Z_0 of the eliminated species is never negligible with respect to X_0^0 and Y_0^0. However this qualitative statement cannot be considered as a criterion to check the validity of the quasi-steady-state approximation, which refers to dynamics and not to steady properties.

The dynamics of the three-variable model depends on the three rate constants k_2', k_{-2}', and k_2'', in addition to the parameters of the two-variable model. We study the behavior of the system in two cuts of the parameter space (k_2', k_{-2}', k_2''). In case a, the parameter k_{-2}' is set at $k_{-2}' = 1$ and k_2' varies with k_2'' according to $k_2' = k_2(1 + k_{-2}'/k_2'')$ in order to obey Eq. (25). Case b corresponds to $k_2' = 10$ and $k_{-2}' = k_2''(-1 + k_2'/k_2)$, which also obeys Eq. (25). We adopt analogous notations as in the two-variable model to characterize the linearized
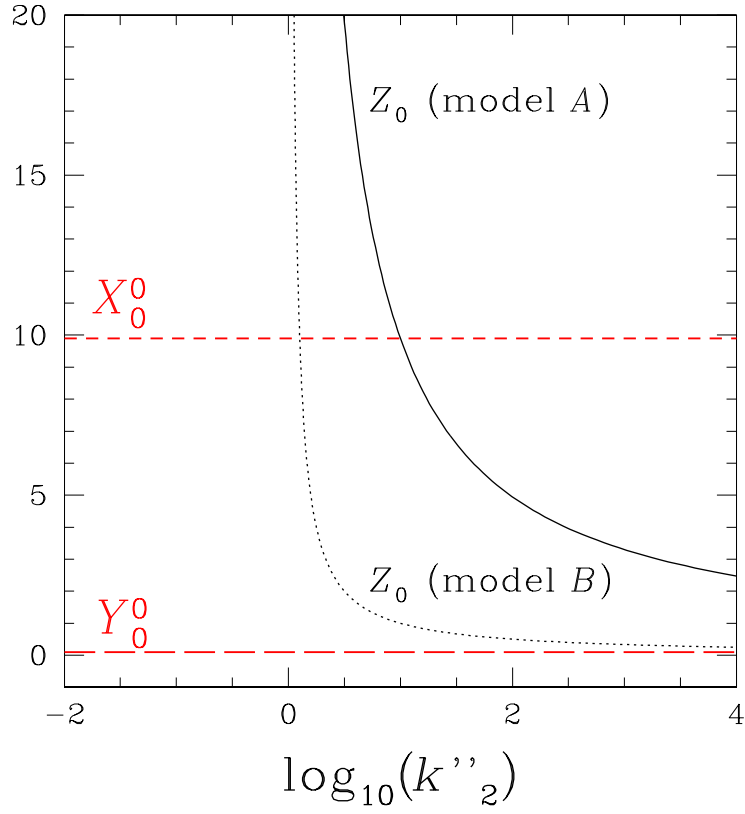
Figure 1: Steady concentrations of species X and Y for the two-variable model and the three-variable models A and B (red short-dashed line for $X_0 = X_0^0$ and red long-dashed line for $Y_0 = Y_0^0$) and steady concentration Z_0 of the three-variable model A (black solid line) and the three-variable model B (black dotted line) versus $\log_{10}(k_2'')$ for $k_1 = k_2 = k_3 = 1$, $k_{-3} = 10$, and $\frac{k_2' k_2''}{k_{-2}' + k_2''} = k_2$.
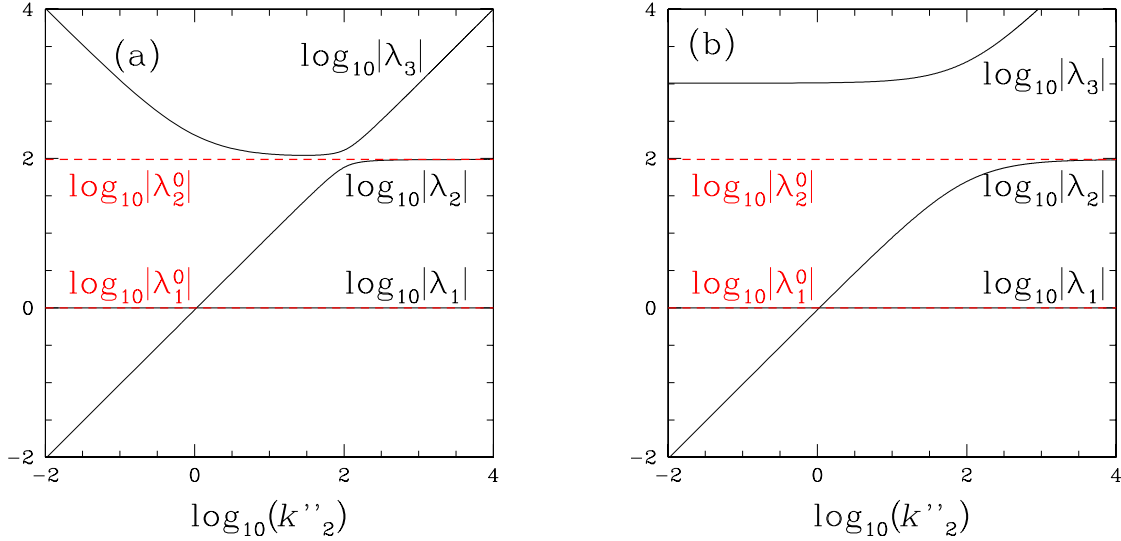
Figure 2: Logarithm of absolute eigenvalues $\log_{10} | \lambda_i^0 |$, $i = 1, 2$, of the two-variable model (red dashed lines) and $\log_{10} | \lambda_i |$, $i = 1, 2, 3$, of the three-variable model A (black solid lines) versus $\log_{10}(k_2'')$ for $k_1 = k_2 = k_3 = 1$, $k_{-3} = 10$. All eigenvalues are real.
(a) Case a: $k_{-2}' = 1$ with $k_2' = k_2(1 + k_{-2}'/k_2'')$. (b) Case b: $k_2' = 10$ with $k_{-2}' = k_2''(-1 + k_2'/k_2)$.

dynamics around the steady state. In particular, the deviations from the steady state are denoted by $x = X - X_0^0$, $y = Y - Y_0^0$, and $z = Z - Z_0$. The matrix form of the linearized equations around the steady state are similar to Eq. (10) with $\zeta = \begin{pmatrix} x \\ y \\ z \end{pmatrix}$ and a 3×3 matrix $\mathbf{M}$ associated with eigenvalues λ_i, with $i = 1, 2, 3$. The vectors $\chi = \begin{pmatrix} x_1 \\ x_2 \\ x_3 \end{pmatrix}$ and ζ are related by $\zeta = \mathbf{P}\chi$, where $\mathbf{P}$ is the 3×3 change of basis matrix. The expressions of the eigenvalues and eigenvectors associated with the three-variable model A are given in Appendix A. The variation of the eigenvalues λ_i, for $i = 1, 2, 3$, versus k_2'' is given in Fig. 2. The eigenvalues λ_1^0 and λ_1 of the two- and three-variable models are identical in the entire k_2'' range. The time $\tau_i = 1/ | R(\lambda_i) |$ associated with the variable x_i characterizes the evolution along the corresponding eigendirection.

In the linear domain around the steady state, the elimination of the variable Z according to the quasi-steady-state approximation can be performed if two conditions are fulfilled.

First, the relaxation in one eigendirection must be particularly fast. This condition implies that the real part of the eigenvalue associated with the fast eigendirection, for example λ_3, must be significantly larger in absolute value than the two others [2, 3, 4]:

$$| R(\lambda_3) |> \max(| R(\lambda_1) |, | R(\lambda_2) |) \tag{29}$$

Second, the coordinate z must vary in the same way as x_3 during the time interval $[0, \tau_3]$. This condition can be expressed using the inverse change of basis matrix $\mathbf{P}^{-1}$

$$x_3 = q_{31}x + q_{32}y + q_{33}z \tag{30}$$

leading to

$$| R(q_{33}) |> \max(| R(q_{31}) |, | R(q_{32}) |) \tag{31}$$

where q_{3i}, for $i = 1, 2, 3$, are the elements of the third line of $\mathbf{P}^{-1}$ and for initial conditions with departures from the steady states x, y, and z of the same order of magnitude. An equivalent condition can be written using the change of basis matrix $\mathbf{P}$, provided that its column vectors, i.e. the eigenvectors, are normalized

$$z = p_{31}x_1 + p_{32}x_2 + p_{33}x_3 \tag{32}$$

which reads

$$| R(p_{33}) |> \max(| R(p_{31}) |, | R(p_{32}) |) \tag{33}$$

where p_{3i}, for $i = 1, 2, 3$, are the elements of the third line of $\mathbf{P}$. Hence, the eigendirections associated with the two small absolute real parts of the eigenvalues are close to the plan $z = 0$. If the two conditions given in Eqs. (29) and (31) are fulfilled, the relaxation with the short characteristic time τ_3 along the x_3-axis can be considered as instantaneous. Further evolution, including Z evolution, occurs with the slower relaxation times on the slow manifold given in Eq. (22). The slow manifold is tangent to the slow eigendirections and is close to the $z = 0$ plane in the vicinity of the steady state.

According to Fig. 2 and for the chosen parameter values, the eigenvalues of the three-variable model A are always real, negative, and obey Eq. (29) except for k_2'' around 100 in case
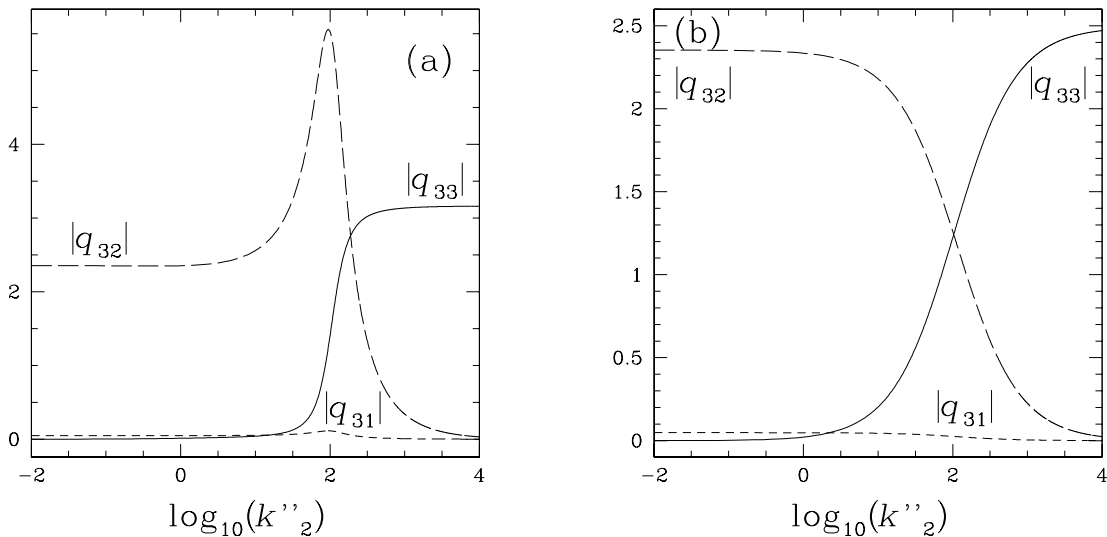
Figure 3: Three-variable model A: Absolute elements $|\,q_{31}\,|$ (short-dashed line), $|\,q_{32}\,|$ (long-dashed lines), and $|\,q_{33}\,|$ (solid line) of the inverse change of basis matrix versus rate constant $\log_{10}(k_2'')$ for the parameter values given in the caption of Fig. 2. (a) Case a and (b) Case b.

a. The variable x_3 of model A which evolves with the characteristic time $\tau_3 = 1/\,|\,R(\lambda_3)\,|$ can be considered as fast with respect to the variables x_1 and x_2 nearly in the entire range of k_2'' values. The eigenvalues λ_1 and λ_2 of the three-variable model A coincide with the eigenvalues λ_1^0 and λ_2^0 of the two-variable system in a smaller interval, $k_2'' > 100$.

Using the vocabulary of quantum chemistry, we notice that an avoided crossing between λ_2 and λ_3 is observed in Fig. 2a for $k_2'' \simeq 100$. The parallelism with a known case of failure of the Born-Oppenheimer approximation can be drawn. Both the quasi-steady-state approximation and the Born- Oppenheimer approximation belong to the class of adiabatic approximations [1]. The Born-Oppenheimer approximation consists in ignoring the fast movements of the electrons and only considering the slow components of their displacements in response to the movement of the nuclei. Introducing a perturbation to the Hamiltonian splits the degenerate energy states and leads to an avoided crossing, exactly as in Fig. 2a when switching from the two-variable model to the three-variable model. The cut of the parameter space associated

with case b does not lead to an avoided crossing for λ_2 and λ_3 as shown in Fig. 2b. It is to be noted that, for $k_2'' = 1$, the crossing of the two eigenvalues λ_1 and λ_2 associated with the slow dynamics is not avoided in model A in both cases a and b.

As shown in Fig. 3, imposing that z evolves like x_3 is more restrictive than Eq. (29). The condition on the elements of $\mathbf{P}^{-1}$ given in Eq. (31) is obeyed for $k_2'' > 10^{2.48}$ in cases a and b. Eq. (33) based on the elements of $\mathbf{P}$ leads to similar results. The avoided crossing of λ_3 and λ_2 observed in Fig. 2a is associated with a maximum for $\mid R(q_{32}) \mid$ in Fig. 3a. We note the absence of both phenomena in Figs. 2b and 3b.

We conclude that the two conditions given in Eqs. (29) and (31) are satisfied in the range $k_2'' > 10^{2.48}$ in which the linear dynamics of the two-variable model and the three-variable model A are close for the two cases a and b. It is worth noting that Eqs. (29) and (31) are only necessary conditions of validity of the quasi-steady-state approximation. But they do not warrant that the two-variable model remains valid when nonlinearities become important, typically when the system is far from the steady state or close to a bifurcation.

2.3   Three-variable model B

The second reaction of the two-variable model can also be decomposed into two reactions involving an intermediate species Z according to

$$\mathrm{X} \xrightarrow{k_1} \mathrm{R}_1 \tag{34}$$

$$\mathrm{X} + \mathrm{Y} \underset{k_{-2}'}{\overset{k_2'}{\rightleftharpoons}} \mathrm{Z} \tag{35}$$

$$\mathrm{X} + \mathrm{Z} \xrightarrow{k_2''} 3\,\mathrm{X} \tag{36}$$

$$\mathrm{Y} \underset{k_{-3}'}{\overset{k_3}{\rightleftharpoons}} \mathrm{R}_2 \tag{37}$$

11

leading to the following differential equations:

$$\frac{\mathrm{d}X}{\mathrm{d}t} = -k_1 X - k_2' XY + k_{-2}' Z + 2k_2'' XZ \tag{38}$$

$$\frac{\mathrm{d}Y}{\mathrm{d}t} = k_{-3} - k_3 Y - k_2' XY + k_{-2}' Z \tag{39}$$

$$\frac{\mathrm{d}Z}{\mathrm{d}t} = k_2' XY - k_{-2}' Z - k_2'' XZ \tag{40}$$

The slow manifold $\frac{\mathrm{d}Z}{\mathrm{d}t} = 0$ is now given by $Z = \frac{k_2' XY}{k_{-2}' + k_2'' X}$. The dynamics on the slow manifold obeys

$$\frac{\mathrm{d}X}{\mathrm{d}t} = -k_1 X + \frac{k_2' k_2''}{k_{-2}' + k_2'' X} X^2 Y \tag{41}$$

$$\frac{\mathrm{d}Y}{\mathrm{d}t} = k_{-3} - k_3 Y - \frac{k_2' k_2''}{k_{-2}' + k_2'' X} X^2 Y \tag{42}$$

which never rigorously converges to the dynamics associated with the two-variable model given in Eqs. (4) and (5). Applying the quasi-steady-state approximation to model B does make it possible to reduce the number of variables. However, due to the nonpolynomial form of Eqs. (41) and (42), the reduced equations cannot be interpreted as rate laws associated with a chemical mechanism involving elementary steps. In particular, the two-variable model defined by Eqs. (1-3) does not account for the nonlinearities of Eqs. (41) and (42) of order higher than 3.

Nevertheless, imposing the relation

$$\frac{k_2' k_2''}{k_{-2}' + k_2'' X_0^0} = k_2 \tag{43}$$

ensures that a steady state of model B obeys

$$X_0 = X_0^0 \tag{44}$$

$$Y_0 = Y_0^0 \tag{45}$$

$$Z_0 = k_1 / k_2'' \tag{46}$$

where (X_0^0, Y_0^0) is the steady state of interest of the two-variable model. The variation of the steady concentrations of model B versus the rate constant k_2'' are given in Fig. 1. As k_2''
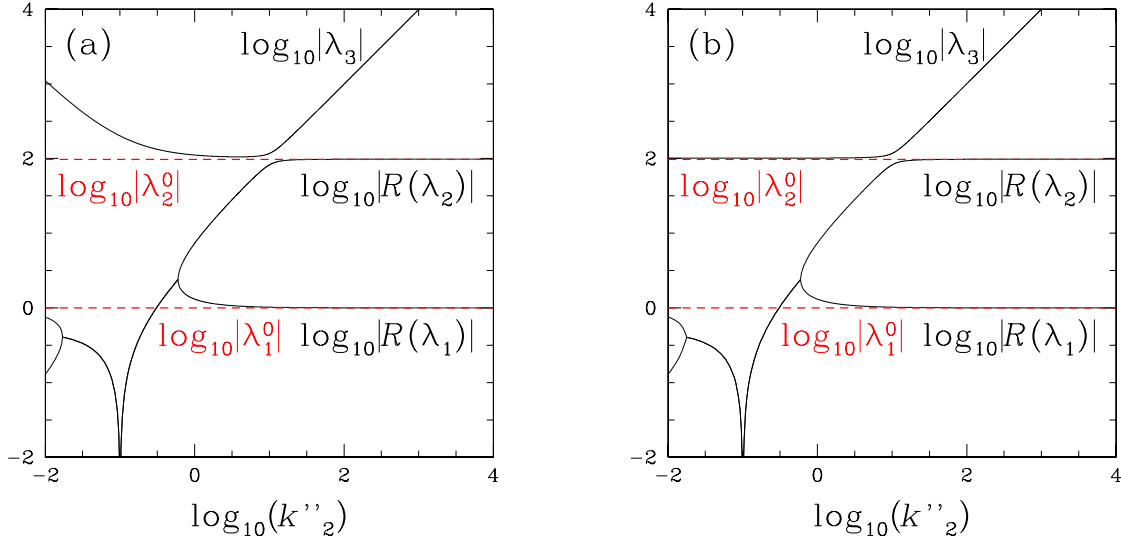
12

Figure 4: Same caption as in Fig. 2 for the three-variable model B using the real part $R(\lambda_i)$ ($i = 1, 2$) of the eigenvalues when they are complex. (a) Case a: $k'_{-2} = 1$ with $k'_2 = k_2(X_0^0 + k'_{-2}/k''_2)$. (b) Case b: $k'_2 = 10$ with $k'_{-2} = k''_2(-X_0^0 + k'_2/k_2)$.

increases, the value of Z_0 decreases earlier in the case of model B than model A, which cannot be considered at this stage as indicating a larger domain of validity of the quasi-steady-state approximation applied to model B.

As shown in Fig. 4ab, the variation of the eigenvalues of the three-variable model B with k''_2 are very similar in the two cases a and b. As k''_2 decreases, several bifurcations are observed. Three real eigenvalues are observed in the range $k''_2 > 10^{-0.22}$. As for model A, the two eigenvalues λ_1 and λ_2 coalesce for $k''_2 = 10^{-0.22}$. Only two real parts of eigenvalues are observed in the range $10^{-1.75} < k''_2 < 10^{-0.22}$ revealing the existence of two complex conjugate eigenvalues λ_1 and λ_2. As k''_2 becomes smaller than 0.1, the real part of λ_1 and λ_2 becomes positive, as evidenced by the divergence of the logarithm of $\mid R(\lambda_1) \mid = \mid R(\lambda_2) \mid$ observed for $k''_2 = 0.1$. The steady state (X_0^0, Y_0^0, Z_0) is then unstable. Another bifurcation occurs for $k''_2 \simeq 10^{-1.75}$, for which the eigenvalues become real again but remain negative. If one excepts the neighborhood of $k''_2 = 10$ for which the orders of magnitude of λ_2 and λ_3 are comparable, model B obeys the condition given in Eq. (29) in the entire range of explored k''_2 values. The
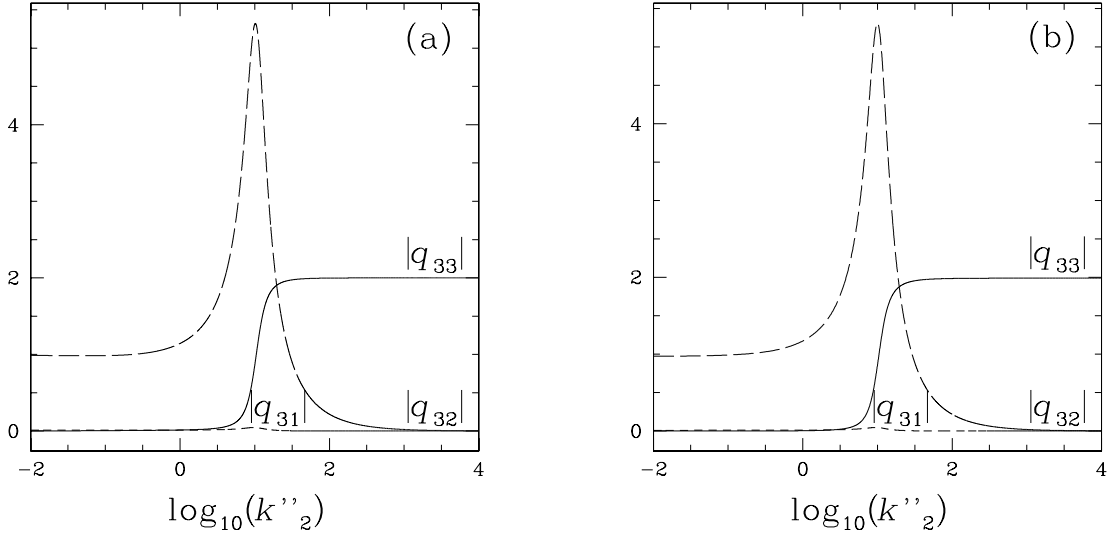
Figure 5: Same caption as in Fig. 3 for the three-variable model B. (a) Case a: $k'_{-2} = 1$ with $k'_2 = k_2(X_0^0 + k'_{-2}/k''_2)$. (b) Case b: $k'_2 = 10$ with $k'_{-2} = k''_2(-X_0^0 + k'_2/k_2)$.

two eigenvalues λ_1^0 and λ_2^0 of the two-variable model coincide with the eigenvalues λ_1 and λ_2 of the three-variable model B if $k''_2 > 10$ in the two cases a and b.

According to Fig. 5, the variation of the elements of the inverse change of basis matrix versus k''_2 are similar for the two cases a and b. The avoided crossing between λ_2 and λ_3 observed in Fig. 4ab reveals that x_2 and x_3 evolve with analogous characteristic times and Eq. (29) is not obeyed for $k''_2 \simeq 10$. This phenomenon is accompanied by a high peak for $\mid R(q_{32}) \mid$ and a significant departure from the condition given in Eq. (31). The condition imposing that the variable z behaves like the fast variable x_3 is obeyed in the range $k''_2 > 10^{1.48}$. Following the linear analysis, we conclude that the quasi-steady-state approximation is valid in the range $k''_2 > 10^{1.48}$ for the three-variable model B in the two cases a and b.

3   Stochastic descriptions

The effect of internal noise in a chemical system can be modeled in an approximate way within the framework of Langevin equations using the expressions of the Langevin forces deduced from the chemical master equation [30, 23]. In this section, we consider Langevin

14

equations linearized in the vicinity of the steady state to compute approximate analytical expressions of variances and covariance of fluctuations for the slow concentrations X and Y. The method is illustrated in the case of the two-variable model. The Langevin equations are integrated in the eigenbasis. The inverse change of basis and the large-time limit are then used to find the steady variances of the concentrations [20, 21, 22]. Deriving the corresponding expressions for the three-variable models is more tedious but follows the same intuitive procedure. The results are given in Appendix B. Another method, using an implicit matrix equation for the variances, is proposed by Gardiner [30] and leads to analogous results.

The linearized Langevin equations for the two-variable model are written as

$$\frac{\mathrm{d}x}{\mathrm{d}t} = m_{11}x + m_{12}y + \frac{1}{\sqrt{\Omega}}\xi_x(t) \tag{47}$$

$$\frac{\mathrm{d}y}{\mathrm{d}t} = m_{21}x + m_{22}y + \frac{1}{\sqrt{\Omega}}\xi_y(t) \tag{48}$$

where Ω scales as the system size, m_{ij} are the elements of the matrix $\mathbf{M}$ given in Eq. (11) and $\xi_x(t)$ and $\xi_y(t)$ are zero-mean Langevin forces. Due to the linearization of the Langevin equations, we have $\langle X \rangle = X_0^0$ and $\langle Y \rangle = Y_0^0$ and $\langle x \rangle = \langle y \rangle = 0$. The variances and covariance of the Langevin forces evaluated at the steady state are given by

$$\langle \xi_x(t)\xi_x(t') \rangle = F_{xx}\delta(t - t') \tag{49}$$

$$\langle \xi_x(t)\xi_y(t') \rangle = F_{xy}\delta(t - t') \tag{50}$$

$$\langle \xi_y(t)\xi_y(t') \rangle = F_{yy}\delta(t - t') \tag{51}$$

with [19]

$$F_{xx} = k_1 X_0^0 + k_2 (X_0^0)^2 Y_0^0 \tag{52}$$

$$F_{xy} = -k_2 (X_0^0)^2 Y_0^0 \tag{53}$$

$$F_{yy} = k_2 (X_0^0)^2 Y_0^0 + k_3 Y_0^0 + k_{-3} \tag{54}$$

Using the change of basis matrix $\mathbf{P^0}$ given in Eq. (14), we determine the scaled variances

and covariance

$$\Omega\langle x^2\rangle = (p_{11}^0)^2 F_{11} + 2p_{11}^0 p_{12}^0 F_{12} + (p_{12}^0)^2 F_{22} \tag{55}$$

$$\Omega\langle xy\rangle = p_{11}^0 p_{21}^0 F_{11} + (p_{11}^0 p_{22}^0 + p_{12}^0 p_{21}^0) F_{12} + p_{12}^0 p_{22}^0 F_{22} \tag{56}$$

$$\Omega\langle y^2\rangle = (p_{21}^0)^2 F_{11} + 2p_{21}^0 p_{22}^0 F_{12} + (p_{22}^0)^2 F_{22} \tag{57}$$

with

$$F_{ij} = \frac{q_{i1}q_{j1}F_{xx} + (q_{i1}q_{j2} + q_{i2}q_{j1})F_{xy} + q_{i2}q_{j2}F_{yy}}{-\lambda_i - \lambda_j} \tag{58}$$

where $i, j = 1, 2$ and the q_{ij}'s are the elements of the inverse matrix of $\mathbf{P}$.

The chemical master equation for the two-variable model is [5, 30]

$$\begin{aligned}
\frac{\partial P}{\partial t} = {} & k_1\big[(N_X + 1)P(\{N_X + 1\}) - N_X P\big] \\
& + \frac{k_2}{\Omega^2}\big[(N_X - 1)(N_X - 2)(N_Y + 1)P(\{N_X - 1, N_Y + 1\}) - N_X(N_X - 1)N_Y P\big] \\
& + k_3\big[(N_Y + 1)P(\{N_Y + 1\}) - N_Y P\big] + k_{-3}\Omega\big[P(\{N_Y - 1\}) - P\big]
\end{aligned} \tag{59}$$

for N_X and N_Y particles of species X and Y at time t in a system of size Ω. Only the dependence of the probability P on the number of particles X and Y differing from N_X and N_Y, respectively, is explicitly indicated. The kinetic Monte Carlo algorithm developed by Gillespie [23] is used to directly simulate the reaction processes and numerically solve the master equation for a system prepared in the steady state with $N_X(t = 0) = \Omega X_0^0$ and $N_Y(t = 0) = \Omega Y_0^0$. The scaled variances $\Omega\langle(N_X - \langle N_X\rangle)^2\rangle$ and $\Omega\langle(N_Y - \langle N_Y\rangle)^2\rangle$ and the covariance $\Omega\langle(N_X - \langle N_X\rangle)(N_Y - \langle N_Y\rangle)\rangle$ of the fluctuations are computed using a statistics over 10^4 realizations.

The master equations associated with the three-variable models are given in Appendix C.

Figure 6ab displays the variation of the scaled variance of the concentration fluctuations of species X versus rate constant k_2'' for the three-variable model A in cases a and b. The variance is multiplied by Ω, so that the scaled results $\Omega\langle x^2\rangle$ deduced from the Langevin
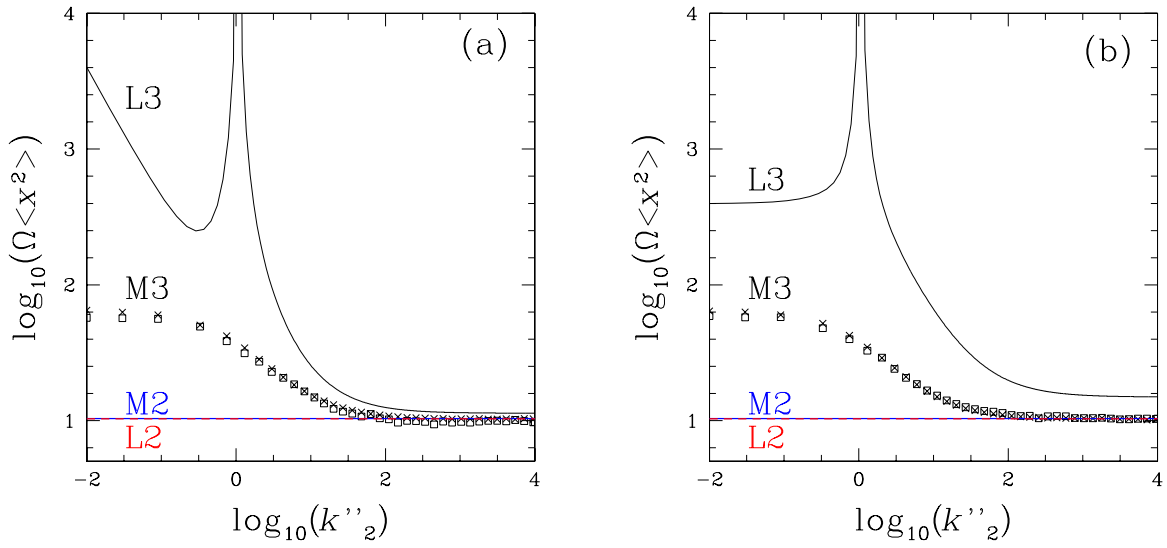
16

Figure 6: Three-variable model A: Logarithm of the scaled variance associated with species X versus $\log_{10}(k_2'')$ for the Langevin approach ($\log_{10}(\Omega\langle x^2\rangle)$, black solid line) and the master equation ($\log_{10}(\Omega\langle(N_X - \langle N_X\rangle)^2\rangle)$) for $\Omega = 3$ ($\square$) and $\Omega = 1000$ ($\times$). Two-variable model: The red dashed line gives the results of the Langevin approach and the blue solid line, the results of the master equation for $\Omega = 1000$. The other parameter values are given in the caption of Fig. 2. (a) Case a and (b) Case b.

approach (see Eq. (73)) are not sensitive to system size and more easily compared to the corresponding result, $\Omega\langle(N_X - \langle N_X\rangle)^2\rangle$, deduced from the master equation. The results of the three-variable model A are compared to those of the two-variable model for both stochastic approaches. In the following, we refer to the Langevin approach applied to the two- and three-variable models as L2 and L3, respectively. The master equation applied to the two- and three-variable models is referred to as M2 and M3. Due to the logarithmic scale adopted to represent the large range covered by the L3 results, the L2 and M2 approaches seem to coincide in Fig. 6ab. The results of the master equation applied to the two-variable model depend little on system size Ω at the scale of the figure and only the results obtained for $\Omega = 1000$ are shown. Indeed, the parameter values of the two-variable model are chosen far from any situation associated with large fluctuation effects such as bifurcations. In this kind of situations, the results of the linearized Langevin approach are satisfying and the agreement with the results of the master equation are expected even for quite small system sizes [20, 21, 22].

No appreciable deviation is observed between the M3 results obtained for different values of system size Ω in both cases a and b. At figure scale, the M3 results converge to the L2 and M2 result for large k_2'' values ($k_2'' > 10^{2.48}$) and deviate from it as k_2'' decreases. Typically, for $k_2'' \simeq 1$, the scaled variance deduced from M3 is multiplied by a factor of 3 with respect to the M2 results. When compared to M3, the L3 results are found to markedly overestimate the deviation between the results of the three- and two-variable models in the range $k_2'' < 10$. The L3 results display a spurious divergence for $k_2'' = 1$, in relation to the crossing of the two eigenvalues λ_1 and λ_2 observed in Fig. 2. In spite of the logarithmic scale, a discrepancy between the L3 result and the L2, M2, and M3 results can be observed in the limit of the largest investigated k_2'' values, in particular in Fig. 6b. The discrepancy between the L3 and M3 results has two origins. First, the Langevin approach introduces Gaussian noises, which implies the intrinsic truncation of the cumulants of the probability distribution function to the second order. Second, the analytical expressions of the variances are deduced from the
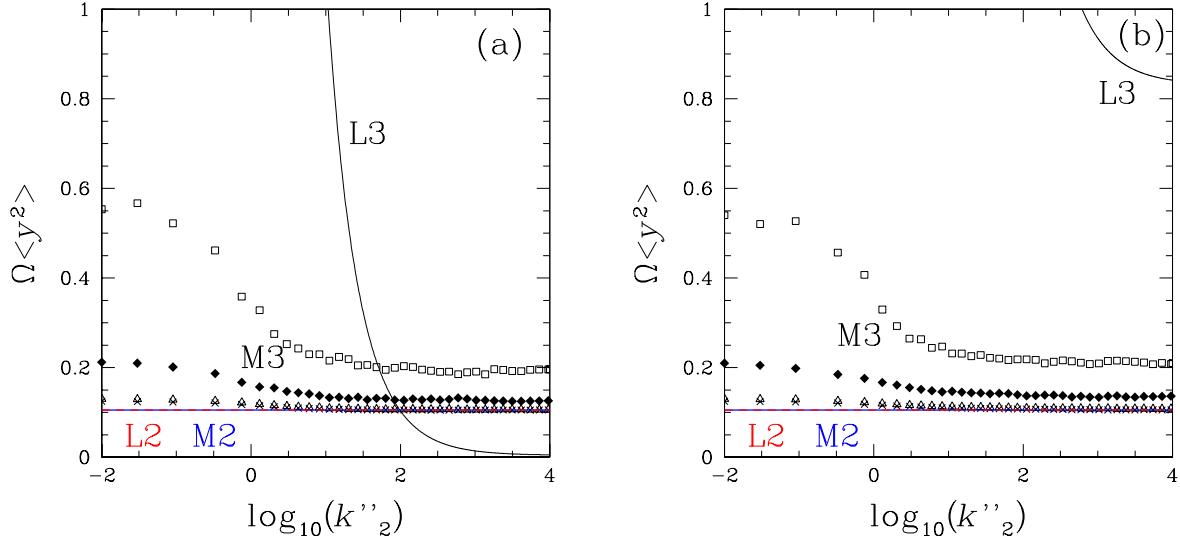
Figure 7: Three-variable model A: Scaled variance associated with species Y versus $\log_{10}(k_2'')$ for the Langevin approach ($\Omega\langle y^2\rangle$, black solid line) and the master equation ($\Omega\langle(N_Y - \langle N_Y\rangle)^2\rangle$) for $\Omega = 3$ ($\square$), $\Omega = 10$ ($\blacklozenge$), $\Omega = 100$ ($\triangle$), and $\Omega = 1000$ ($\times$). Two-variable model: The red dashed line gives the results of the Langevin approach and the blue solid line, the results of the master equation for $\Omega = 1000$. The other parameter values are given in the caption of Fig. 2. (a) Case a and (b) Case b.

linearization of the Langevin equations around the steady state whereas the master equation provides an exact stochastic description at a mesoscopic scale.

The variation of the scaled variance $\Omega\langle y^2\rangle$ or $\Omega\langle(N_Y - \langle N_Y\rangle)^2\rangle$ of the concentration fluctuations of species Y with k_2'' is given in Fig. 7. The two stochastic approaches L2 and M2 for the two-variable model agree. The L3 results are entirely different from both the M3 results and the L2 and M2 results, including in the large k_2'' limit. Contrary to the L3 results, the M3 results are similar in cases a and b. The L3 results significantly deviate from the M3 predictions for $k_2'' < 10^{1.48}$. The M3 results converge towards the L2 and M2 results in the limit of large k_2'', ($k_2'' > 100$), and large system size, ($\Omega \geq 100$). Interestingly, the M3 results obtained for sufficiently small system sizes ($\Omega < 100$) never coincide with the L2 and M2 results: Even in the parameter domain $k_2'' > 10^{1.48}$, where the quasi-steady-state approximation is valid from the deterministic point of view, the behavior of the variance of
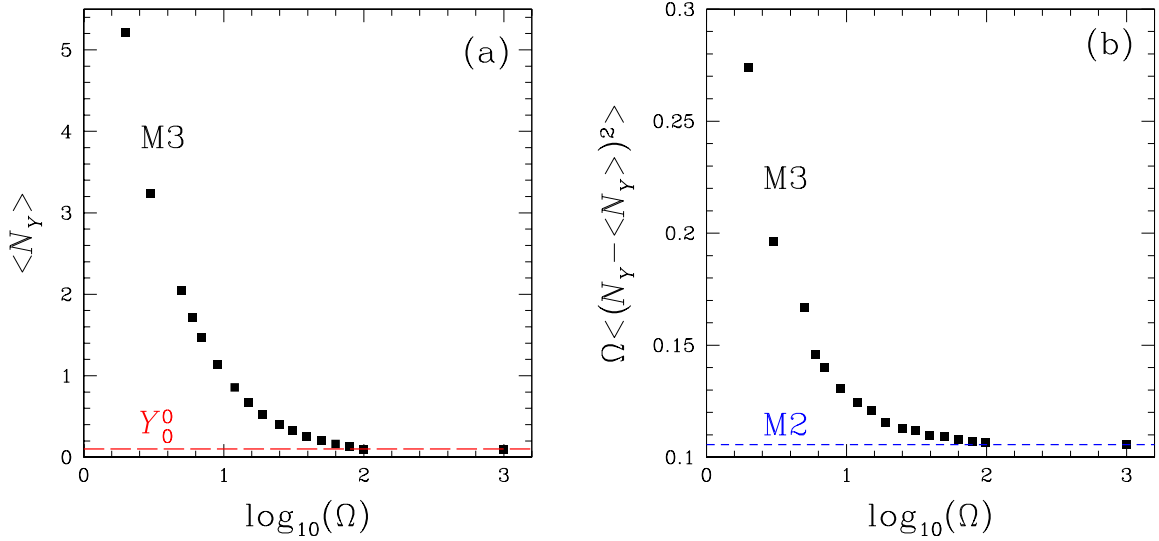
Figure 8: Three-variable model A in case a for $k_2'' = 10^4$: (a) Mean value $\langle N_Y \rangle$ deduced from the master equation (■) and deterministic prediction Y_0^0 (red long-dashed line) versus $\log_{10}(\Omega)$. (b) Scaled variance $\Omega \langle (N_Y - \langle N_Y \rangle)^2 \rangle$ deduced from the master equation for the three-variable model A (■) and the two-variable model (blue short-dashed line) versus $\log_{10}(\Omega)$. The other parameter values are given in the caption of Fig. 2a.

species Y in the three-variable model significantly differs from the behavior obtained in the two-variable model.

The effect is more marked in the case of species Y than species X, due to the smaller value of the steady concentration Y_0^0: A concentration being a positive variable, the fluctuations around the mean value become asymmetrical when they reach the order of Y_0^0, i.e. for a sufficiently small system size Ω. As shown in Fig. 8, this phenomenon leads to the increase of the scaled variance $\Omega \langle (N_Y - \langle N_Y \rangle)^2 \rangle$ as Ω decreases. In addition, the mean value $\langle N_Y \rangle$ is shifted from the deterministic steady state Y_0^0.

The scaled covariance $\Omega \langle xy \rangle$ or $\Omega \langle (N_X - \langle N_X \rangle)(N_Y - \langle N_Y \rangle) \rangle$ associated with species X and Y is represented in Fig. 9. In case a, the results of the two stochastic approaches for the three-variable model converge toward the results obtained for the two-variable model in the limit of large k_2''. However, as k_2'' becomes smaller than 1000, the L3 results increase and even
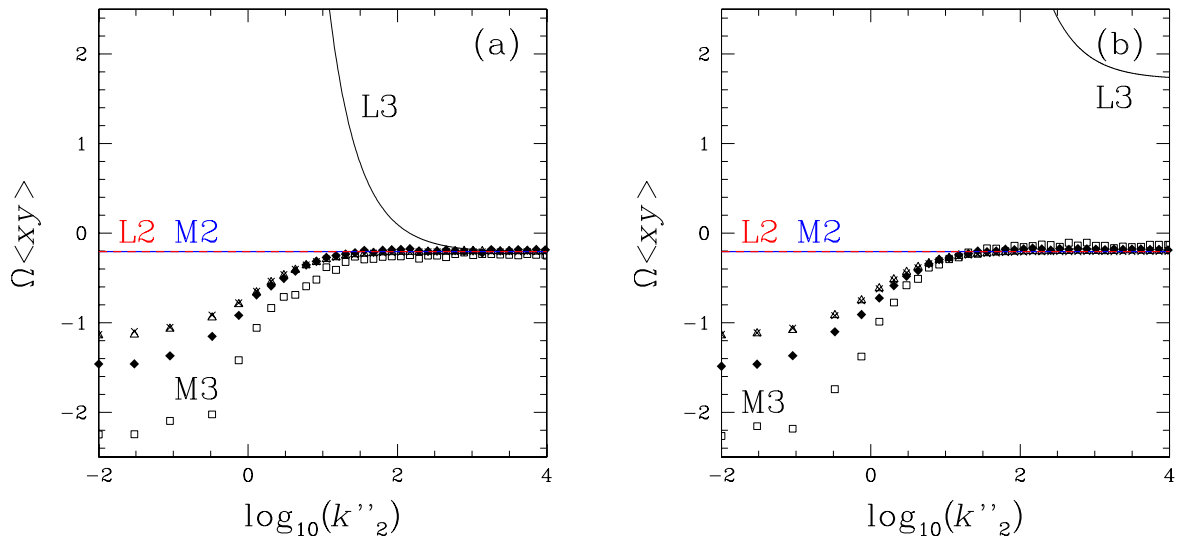
Figure 9: Three-variable model A: Same caption as in Fig. 7 for the scaled covariance $\Omega\langle xy\rangle$ (Langevin approach) or $\Omega\langle(N_X - \langle N_X\rangle)(N_Y - \langle N_Y\rangle)\rangle$ (master equation). (a) Case a and (b) Case b.

become positive whereas the M3 results decrease and begin to appreciably depart from the M2 results only as k_2'' becomes smaller than 10. In case b, the L3 results are always far from the L2 results. As shown in Fig. 2, the convergence of the eigenvalue λ_2 of the three-variable model A toward the corresponding eigenvalue λ_2^0 of the two-variable model as k_2'' increases is slower in case b than in case a. Similarly, the increase of the absolute element $\mid q_{33} \mid$ as k_2'' increases is slower in case b than in case a, as observed in Fig. 3. This could explain that, for large values of k_2'', the Langevin approach L3 is more different from L2 in case b than in case a in Figs. 6, 7, and 9. The master equation approach is less sensitive to this feature. Only a small increase of the M3 results with respect to the M2 results is detectable in Fig. 9b in the limit of large k_2'' for a small system size $\Omega = 3$, whereas the corresponding L3 results are much larger than the L2 results. These observations suggest that the nonlinearities ignored in the linearized Langevin approach mitigate the effect of the discrepancies between the eigenvalues of the two- and three-variable models. The sign of the covariance can be easily deduced for the two-variable model, in which the second reaction given in Eq. (2) forms species X and consumes species Y: The covariance is negative. The situation is different for

21

the three-variable model A, in which both species X and Y are consumed (formed, resp.) by the forward (backward, resp.) reaction given in Eq. (16) whereas only X is formed by the third reaction given in Eq. (17). According to Fig. 9, the master equation approach M3 captures the sign of the covariance even for small values of k_2'' for which the elimination of Z is not valid whereas L3 fails.

Figures 10-12 give the variances and covariance of the fluctuations of the slow variables X and Y for the three-variable model B. Due to the similarity of the behaviors observed in cases a and b, only case a is represented. The results of the stochastic approaches are not given in the parameter domain $k_2'' < 0.1$ in which the steady state is unstable, as shown in Fig. 4a.

According to Fig. 10, the scaled variance $\Omega\langle x^2 \rangle$ deduced from L2 is slightly smaller than the result deduced from M2. The small gap between L2 and M2 results could not be seen in Fig. 6 due to the adopted logarithmic scale. The L3 results of the Langevin approach applied to the three-variable model completely differ from the L2 predictions in the entire range of k_2'': The L3 limit at large k_2'' underestimates the L2 value by a factor of 1.6 and the spurious divergence observed for $k_2'' = 0.6$ due to the coalescence of the eigenvalues λ_1 and λ_2 (see Fig. 4) induces a rapid increase of $\Omega\langle x^2 \rangle$ in the range $10^{-0.22} < k_2'' < 100$. The M3 results for the scaled variance $\Omega\langle (N_X - \langle N_X \rangle)^2 \rangle$ do not converge toward the M2 results even in the limit of large k_2'' and Ω. The fact that, for the same parameter values, Z_0 is smaller in the case of model B than model A (see Fig. 1) is not sufficient to ensure the matching between the stochastic predictions of the two-variable model and three-variable model B. Indeed, the nonlinearities observed in the rate laws (see Eqs. (41) and (42)) after applying the quasi-steady-state approximation to model B are different from the nonlinearities present in the original two-variable model. The nonconvergence of the M3 results toward the M2 results at large k_2'' and Ω in the case of model B illustrates the decisive role played by the nonlinearities of the deterministic dynamics in fluctuation properties.
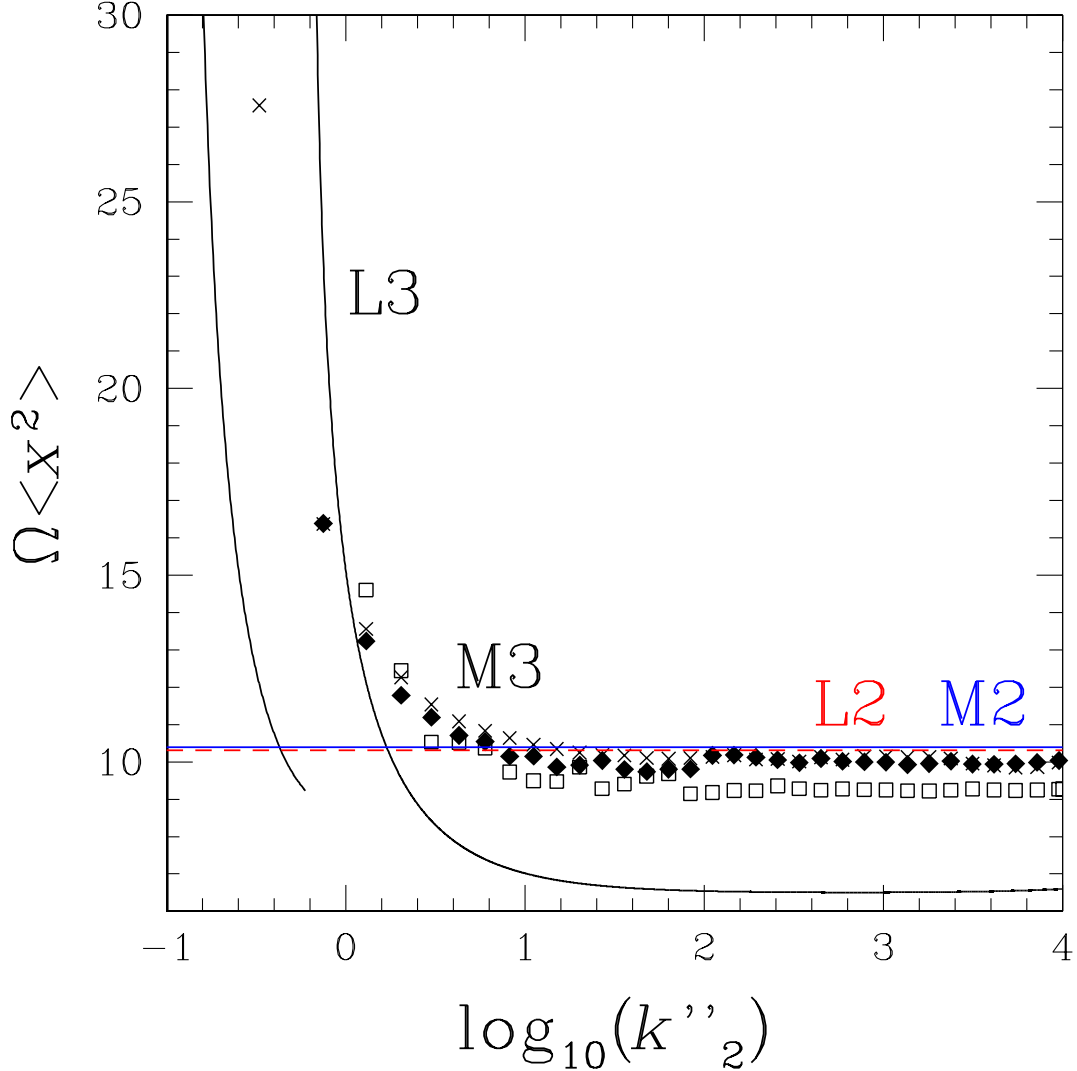
Figure 10: Three-variable model B in case a: Scaled variance associated with species X versus $\log_{10}(k_2'')$ for the Langevin approach ($\Omega\langle x^2\rangle$, black solid line) and the master equation ($\Omega\langle(N_X - \langle N_X\rangle)^2\rangle$) for $\Omega = 3$ ($\square$), $\Omega = 10$ ($\blacklozenge$), and $\Omega = 1000$ ($\times$). Two-variable model: The red dashed line gives the results of the Langevin approach and the blue solid line, the results of the master equation for $\Omega = 1000$. Case a: $k_{-2}' = 1$ with $k_2' = k_2(X_0^0 + k_{-2}'/k_2'')$. The other parameter values are given in the caption of Fig. 2.
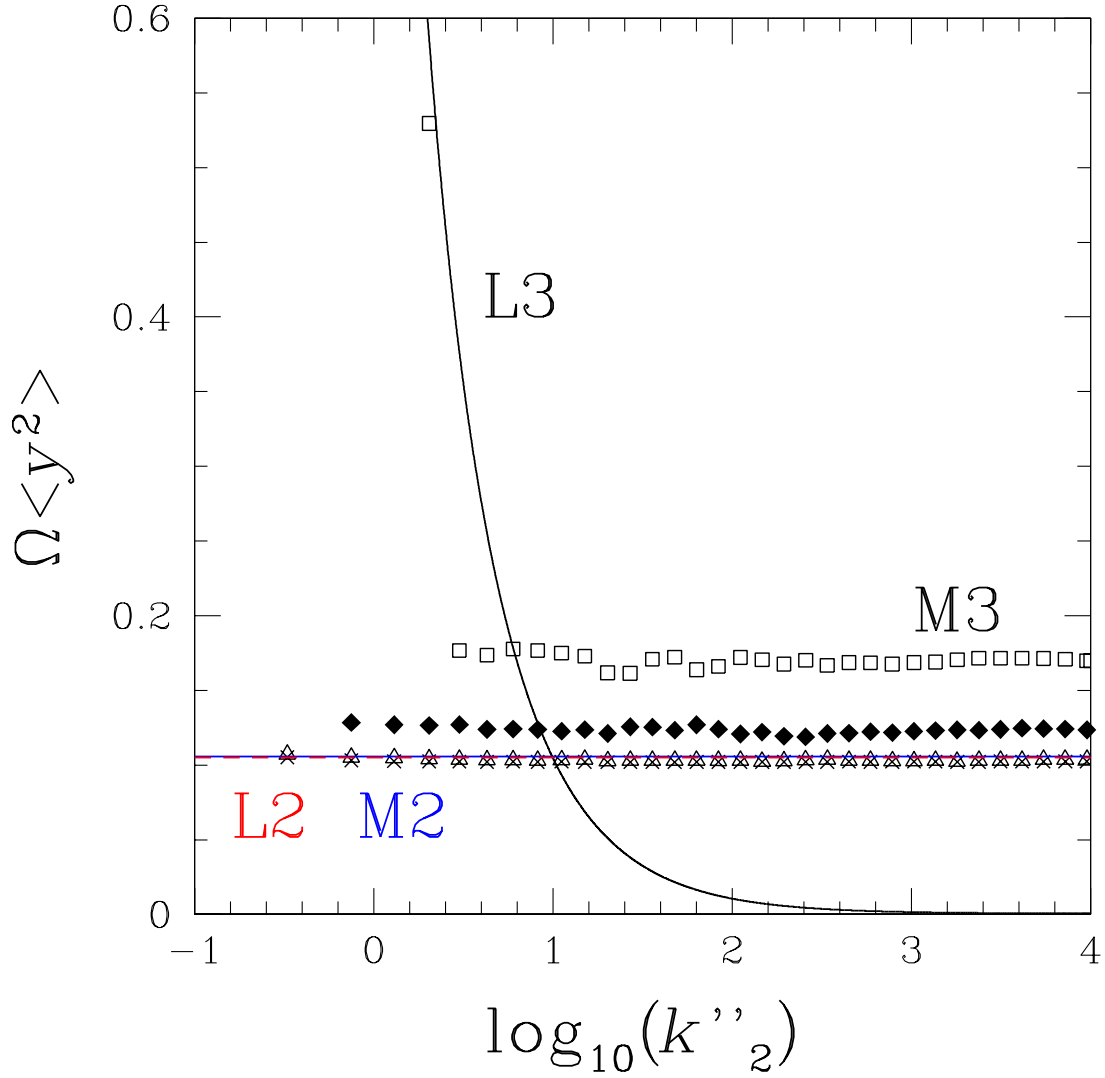
Figure 11: Three-variable model B: Same caption as in Fig. 10 for the scaled variance $\Omega\langle y^2\rangle$ (Langevin approach) or $\Omega\langle(N_Y - \langle N_Y\rangle)^2\rangle$ (master equation) associated with species Y.

The sensitivity of the M3 results to system size for species X in Fig. 10 is small, compared to the results observed in Fig. 11 for species Y. As already mentioned, the sensitivity of $\Omega\langle(N_Y - \langle N_Y\rangle)^2\rangle$ to Ω is related to the small value of Y_0^0 which induces asymmetrical fluctuations around the mean value for sufficiently small system sizes. The results given in Fig. 11 for model B are qualitatively the same as those given in Fig. 7 for model A.

The results obtained for the covariance in the case of model B are given in Fig. 12. Contrary to model A (see Fig. 9) for which the results of the master equation converge toward the L2 and M2 limit at large k_2'', the M3 results obtained for model B remain larger than the L2 and M2 limit, even for a large system size $\Omega = 1000$. The covariance deduced from the M3 approach decreases as k_2'' tends to the critical value $k_2'' = 0.1$ below which the steady state becomes unstable.

Although the three-variable models A and B converge to the same deterministic two-variable model, at least for the steady properties and linear dynamics, the variances and covariance of the slow variables in models A and B have different behaviors. Hence, the proper description of the fluctuations in models A and B by the two-variable model deduced from the steady-state-approximation is not ensured in systems of small size. Sizes of the order of $\Omega = 1000$ have to be reached for the results of the master equation applied to the three-variable models to converge toward the results of the two-variable model.

4   Discussion and conclusion

In this paper, we introduce a fast species in a chemical mechanism and show that it perturbs the fluctuations of the slow species even in the domain of validity of the quasi-steady-state approximation, in which the deterministic dynamics is correctly predicted by the reduced mechanism in the linear domain.

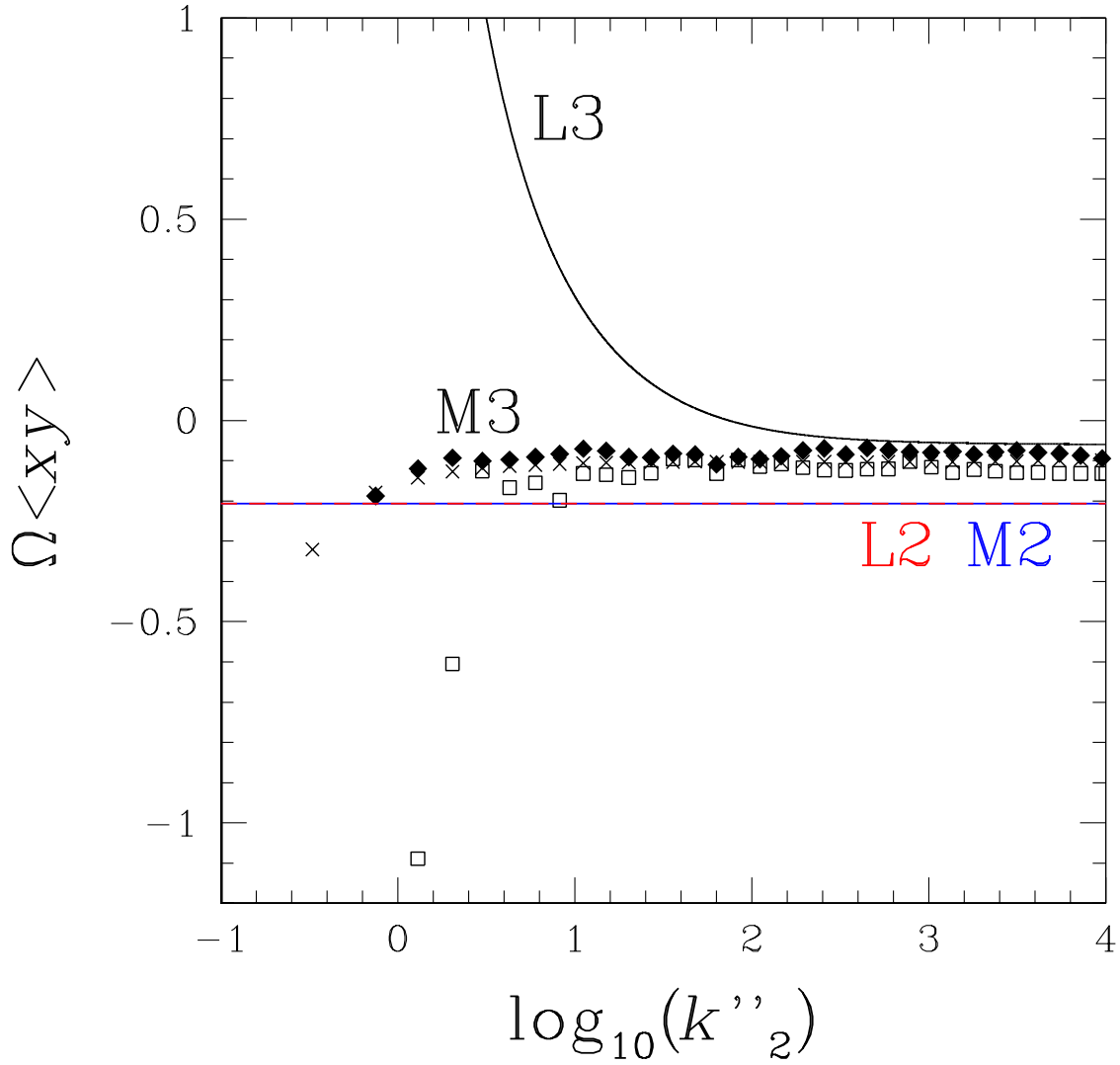The study provides an opportunity to revisit the quasi-steady-state approximation. By

Figure 12: Three-variable model B: Same caption as in Fig. 10 for the scaled covariance $\Omega\langle xy\rangle$ (Langevin approach) or $\Omega\langle(N_X - \langle N_X\rangle)(N_Y - \langle N_Y\rangle)\rangle$ (master equation).

completely neglecting fast relaxation and restricting the dynamics to the slow manifold, the approximation can be considered as a zeroth-order perturbation method, which masks the small parameter and makes the definition of the validity domain less obvious.

The existence of a fast variable is sufficient to reduce dynamics but, in the general case, the slow variables are non trivial functions of the entire set of the initial variables, e.g. a linear combination of all concentrations in the framework of a linear analysis. The quasi-steady-state approximation eliminates a chemical species and consequently requires that the fast variable is close to an actual concentration. In the linear domain, characteristic relaxation times are assigned to the evolution along eigendirections and the notion of fast or slow variables to coordinates in the eigenbasis. We express the conditions of validity of the approximation using the eigenvalues and appropriate elements of the change of basis matrix. The parallelism with the Born-Oppenheimer approximation in quantum chemistry is drawn, in particular in the case of avoided crossing between two eigenvalues.

The approximation is applied to two three-variable models A and B and the possible reduction to a same two-variable model is discussed. Conditions on the parameters of the three-variable models are made explicit for the two- and three-variable models to have the same steady state of interest. Model B offers a simple example showing that small concentrations for a slowly formed and rapidly consumed species cannot be considered as a valid condition of elimination. The intuitive belief used to eliminate a very reactive intermediate from a mechanism coincides with the dynamical criteria made precise in section 2 in the case of intrinsically linear dynamics but not in general. In the case of model A, the steady value $Z_0 \simeq 2.5$ of the eliminated variable Z that is reached for $k_2'' = 10^4$ is already reached for $k_2'' = 10^{0.3}$ in the case of model B. According to the master equation and for a given value of Z_0, the deviations of the variances and covariance in the three-variable models to the corresponding quantities in the two-variable model are smaller for model A than model B. More precisely, for a large system size, $\Omega = 1000$, the M3 value of the variance $\Omega \langle (N_X - \langle N_X \rangle)^2 \rangle$ in model A for $k_2'' = 10^4$ underestimates the M2 value by less than 1%

whereas the corresponding result associated with the same Z_0 value in model B, i.e. for $k_2'' = 10^{0.3}$, overestimates the M2 value by 18%. Similarly, the M3 result for the covariance $\Omega\langle(N_X - \langle N_X \rangle)(N_Y - \langle N_Y \rangle)\rangle$ in model A for $k_2'' = 10^4$ overestimates the M2 value by only 0.6% whereas the corresponding result in the case of model B for $k_2'' = 10^{0.3}$ overestimates the M2 value by 38%. The larger discrepancies between M3 and M2 results in the case of model B for the same value of Z_0 are related to the specific nonlinearities introduced in the macroscopic rate equations when eliminating the fast variable Z. These nonpolynomial non-linearities differ from the nonlinearities of the two-variable model and the interplay between the nonlinearities of the deterministic dynamics and the fluctuations is known to be complex and model specific [20, 21, 22]. The two-variable mechanism does not correctly account for the nonlinearities of the reduced dynamics of the three-variable model B and can only claim to model the linearized properties of the three-variable model around the steady state. The reduction of a mechanism often leads to such nonpolynomial nonlinearities, as for example in the case of the reduced Michaelis-Menten scheme [31]. Our results show that the conclusions that could be deduced from a stochastic analysis relying on the reduced Michaelis-Menten model may differ from the direct analysis of the complete scheme.

In the parameter range in which the reduction of the deterministic dynamics is valid in the linear domain and for both three-variable models A and B, the variances and covariance of the fluctuations of the slow concentrations do not always coincide with the corresponding quantities obtained for the two-variable model. The deficiencies of the linearized Langevin approach in capturing the properties of the internal fluctuations in a nonlinear chemical system and the necessary resort to the master equation are pointed out. Even the sign of the covariance of the fluctuations is not always correctly predicted by the Langevin equa-tions. The small value Y_0^0 of the steady concentration of species Y inducing asymmetrical fluctuations, the variance of the Y-fluctuations deduced from both three-variable models sig-nificantly depends on system size and differs from the prediction of the two-variable model for

sufficiently small system sizes leading to fluctuation amplitudes larger than Y_0^0. The variance of the fluctuations around the large steady concentration X_0^0 deduced from the three-variable model B is not very sensitive to system size but does not converge toward the prediction of the two-variable model. We already pointed out the differences between the nonlinearities of the reduced dynamics obtained for model B and those of the two-variable model of reference. The coupling between the fluctuations and the nonlinearities of deterministic dynamics makes the use of the quasi-steady-state approximation delicate when the studied system requires a good control. The predictions of a reduced mechanism must be considered with special care when modeling pattern formation in biology, preventing hazards in explosive phenomena, or dealing with small systems in which variances of fluctuations are detected as in fluorescence correlation spectroscopy (FCS).

A   Eigenvalues and eigenbasis of the three-variable models

The eigenvalues of the three-variable models are solution to a cubic polynomial, determined through the Cardano's method. In the case of the three-variable model A, the stability matrix $\mathbf{M}$ is

$$\mathbf{M} = \begin{pmatrix} m_{11} = -(4k_2'X_0^0Y_0^0 + k_1) & m_{12} = -2k_2'(X_0^0)^2 & m_{13} = 2k_{-2}' + 3k_2'' \\ m_{21} = -2k_2'X_0^0Y_0^0 & m_{22} = -(k_2'(X_0^0)^2 + k_3) & m_{23} = k_{-2}' \\ m_{31} = 2k_2'X_0^0Y_0^0 & m_{32} = k_2'(X_0^0)^2 & m_{33} = -(k_{-2}' + k_2'') \end{pmatrix} \quad (60)$$

with X_0^0, Y_0^0 given in Eqs. (8) and (9).

For the three-variable model B, the linear stability operator $\mathbf{M}$ is

$$\mathbf{M} = \begin{pmatrix} m_{11} = -k_2'Y_0^0 - k_1 + 2k_2''Z_0 & m_{12} = -k_2'X_0^0 & m_{13} = k_{-2}' + 2k_2''X_0^0 \\ m_{21} = -k_2'Y_0^0 & m_{22} = -(k_2'X_0^0 + k_3) & m_{23} = k_{-2}' \\ m_{31} = k_2'Y_0^0 - k_2''Z_0 & m_{32} = k_2'X_0^0 & m_{33} = -(k_{-2}' + k_2''X_0^0) \end{pmatrix} \quad (61)$$

where the steady concentrations X_0^0, Y_0^0 are given in Eqs. (8) and (9) and Z_0 is given in Eq. (46).

Following Cardano's method, we set for each three-variable model

$$a = 1, \quad b = -(m_{11} + m_{22} + m_{33}), \tag{62}$$

$$c = -m_{12}m_{21} - m_{13}m_{31} - m_{23}m_{32} + m_{11}m_{22} + m_{11}m_{33} + m_{22}m_{33}, \tag{63}$$

$$d = m_{11}(m_{23}m_{32} - m_{22}m_{33}) + m_{21}(m_{12}m_{33} - m_{13}m_{32}) + m_{31}(m_{13}m_{22} - m_{12}m_{23}) \tag{64}$$

$$e = -\frac{b^2}{3a^2} + \frac{c}{a}, \tag{65}$$

$$f = \frac{b}{27a}\left(2\frac{b^2}{a^2} - 9\frac{c}{a}\right) + \frac{d}{a}, \quad \delta = -(4e^3 + 27f^2) \tag{66}$$

If $\delta \geq 0$, we set

$$u^3 = \frac{-f + i\sqrt{\delta/27}}{2}, \quad v^3 = \frac{-q - i\sqrt{\delta/27}}{2} \tag{67}$$

and if $\delta < 0$, we write

$$u^3 = \frac{-f + \sqrt{-\delta/27}}{2}, \quad v^3 = \frac{-q - \sqrt{-\delta/27}}{2} \tag{68}$$

The eigenvalues of the 3×3 matrix $\mathbf{M}$ are given by

$$\lambda_1 = \ell u + \bar{\ell} v - \frac{b}{3a} \tag{69}$$

$$\lambda_2 = u + v - \frac{b}{3a} \tag{70}$$

$$\lambda_3 = \bar{\ell} u + \ell v - \frac{b}{3a} \tag{71}$$

where $\ell = -1/2 + i\sqrt{3}/2$.

The jth eigenvector, i.e., the jth column $\mathbf{P}_j$ for $j = 1, 2, 3$ of the change of basis matrix $\mathbf{P}$ can also be written in a form valid for both three-variable models

$$\mathbf{P}_j = \begin{pmatrix} p_{1j} = 1 \\ p_{2j} = \frac{\lambda_j - m_{11} - m_{13}p_{31}}{m_{12}} \\ p_{3j} = \frac{(\lambda_j - m_{11})(\lambda_j - m_{22}) - m_{12}m_{21}}{m_{13}(\lambda_j - m_{22}) + m_{12}m_{23}} \end{pmatrix} \tag{72}$$

where the eigenvalues λ_j are given in Eqs. (69-71) and the elements m_{ij} are given in Eq. (60) for model A and Eq. (61) for model B.

B Variances and covariance of concentration fluctuations in the three-variable models deduced from the Langevin equations

Extending the approach given in section 3 for a two-variable system to three-variable systems, we obtain the scaled variances and covariance of the deviations x and y to the steady concentrations X_0^0 and Y_0^0

$$\Omega\langle x^2 \rangle = (p_{11})^2 F_{11} + (p_{12})^2 F_{22} + (p_{13})^2 F_{33} + 2p_{11}p_{12}F_{12} + 2p_{11}p_{13}F_{13} + 2p_{12}p_{13}F_{23} \quad (73)$$

$$\Omega\langle y^2 \rangle = (p_{21})^2 F_{11} + (p_{22})^2 F_{22} + (p_{23})^2 F_{33} + 2p_{21}p_{22}F_{12} + 2p_{21}p_{23}F_{13} + 2p_{22}p_{23}F_{23} \quad (74)$$

$$\Omega\langle xy \rangle = p_{11}(p_{21}F_{11} + p_{22}F_{12} + p_{23}F_{13}) + p_{12}(p_{21}F_{12} + p_{22}F_{22} + p_{23}F_{23})$$

$$+ p_{13}(p_{21}F_{13} + p_{22}F_{23} + p_{23}F_{33}) \quad (75)$$

with

$$F_{ij} = \frac{q_{i1}(q_{j1}F_{xx} + q_{j2}F_{xy} + q_{j3}F_{xz}) + q_{i2}(q_{j1}F_{xy} + q_{j2}F_{yy} + q_{j3}F_{yz}) + q_{i3}(q_{j1}F_{xz} + q_{j2}F_{yz} + q_{j3}F_{zz})}{-(\lambda_i + \lambda_j)} \quad (76)$$

for $i, j = 1, 2, 3$ and where q_{ij} are the elements of the inverse matrix of the change of basis matrix $\mathbf{P}$ (see Eq. (72)) and the variances and covariances of the Langevin forces are

$$F_{xx} = k_1 X_0^0 + 4k_2'(X_0^0)^2 Y_0^0 + (4k_{-2}' + 9k_2'')Z_0 \quad (77)$$

$$F_{yy} = k_2'(X_0^0)^2 Y_0^0 + k_{-2}' Z_0 + k_3 Y_0 + k_{-3} \quad (78)$$

$$F_{zz} = k_2'(X_0^0)^2 Y_0^0 + (k_{-2}' + k_2'')Z_0 \quad (79)$$

$$F_{xy} = 2k_2'(X_0^0)^2 Y_0^0 + 2k_{-2}' Z_0 \quad (80)$$

$$F_{xz} = -2k_2'(X_0^0)^2 Y_0^0 - (2k_{-2}' + 3k_2'')Z_0 \quad (81)$$

$$F_{yz} = -k_2'(X_0^0)^2 Y_0^0 - k_{-2}' Z_0 \quad (82)$$

in the case of model A and

$$F_{xx} = k_1 X_0^0 + k_2' X_0^0 Y_0^0 + (k_{-2}' + 4k_2'' X_0^0)Z_0 \tag{83}$$

$$F_{yy} = k_2' X_0^0 Y_0^0 + k_{-2}' Z_0 + k_3 Y_0^0 + k_{-3} \tag{84}$$

$$F_{zz} = k_2' X_0^0 Y_0^0 + (k_{-2}' + k_2'' X_0^0)Z_0 \tag{85}$$

$$F_{xy} = k_2' X_0^0 Y_0^0 + k_{-2}' Z_0 \tag{86}$$

$$F_{xz} = -k_2' X_0^0 Y_0^0 - (k_{-2}' + 2k_2'')Z_0 \tag{87}$$

$$F_{yz} = -k_2' X_0^0 Y_0^0 - k_{-2}' Z_0 \tag{88}$$

in the case of model B.

C Master equation of the three-variable models

The master equation associated with the three-variable model A is

$$
\begin{aligned}
\frac{\partial P}{\partial t} =\ & k_1\big[(N_X + 1)P(N_X + 1) - N_X P\big] \\
& + \frac{k_2'}{\Omega^2}\big[(N_X + 2)(N_X + 1)(N_Y + 1)P(N_X + 2, N_Y + 1, N_Z - 1) - N_X(N_X - 1)N_Y P\big] \\
& + k_{-2}'\big[(N_Z + 1)P(N_X - 2, N_Y - 1, N_Z + 1) - N_Z P\big] \\
& + k_2''\big[(N_Z + 1)P(N_X - 3, N_Z + 1) - N_Z P\big] \\
& + k_3\big[(N_Y + 1)P(N_Y + 1) - N_Y P\big] + k_{-3}\Omega\big[P(N_Y - 1) - P\big]
\end{aligned}
\tag{89}
$$

The master equation for model B is

$$
\begin{aligned}
\frac{\partial P}{\partial t} =\ & k_1\big[(N_X + 1)P(N_X + 1) - N_X P\big] \\
& + \frac{k_2'}{\Omega}\big[(N_X + 1)(N_Y + 1)P(N_X + 1, N_Y + 1, N_Z - 1) - N_X N_Y P\big] \\
& + k_{-2}'\big[(N_Z + 1)P(N_X - 1, N_Y - 1, N_Z + 1) - N_Z P\big] \\
& + \frac{k_2''}{\Omega}\big[(N_X - 2)(N_Z + 1)P(N_X - 2, N_Z + 1) - N_X N_Z P\big] \\
& + k_3\big[(N_Y + 1)P(N_Y + 1) - N_Y P\big] + k_{-3}\Omega\big[P(N_Y - 1) - P\big]
\end{aligned}
\tag{90}
$$

Conflicts of interest

There are no conflicts to declare.

5   Acknowledgments

References

[1] N. G. Van Kampen, *Phys. Rep.*, 1985, **124**, 69–160.

[2] L.A. Segel and M. Slemrod, *SIAM Rev.*, 1989, **31**, 446–477.

[3] T. Turanyi, A. S. Tomlin and M. J. Pilling, *J. Phys. Chem.*, 1993, **97**, 163–172.

[4] A. N. Gorban, *Curr. Opin. Chem. Eng.*, 2018, **21**, 48–59.

[5] G. Nicolis and I. Prigogine, *Self-organization in nonequilibrium systems*, Wiley, New York, 1977.

[6] A. M. Turing, *Philos. Trans. R. Soc. London, Ser. B*, 1952, **237**, 37–72.

[7] M. Frankowicz, M. Moreau, P. P. Szczesny, J. Toth and L. Vicente, *J. Chem. Phys.*, 1993, **97**, 1891–1895.

[8] Y. Lan, T. C. Elston and G. A. Papoian, *J. Chem. Phys.*, 2008, **129**, 214115.

[9] N. A. Sinitsyn, N. Hengartner and I. Nemenman, *Proc. Natl Acad. Sci. USA*, 2009, **106**, 10546–10551.

[10] P. Thomas, R. Grima and A. V. Straube, *Phys. Rev. E*, 2012, **86**, 041110.

[11] G. W. A. Constable, A. J. McKane and T. Rogers, *J. Phys. A: Math. Theor.*, 2013, **46**, 295002.

[12] G. W. Constable and A. J. McKane, *Phys. Rev. E*, 2014, **89**, 032141.

[13] H. Qian and E. L. Elson, *Proc. Natl. Acad. Sci. USA*, 2004, **101**, 2828–2833.

[14] S. Charier, A. Meglio, D. Alcor, E. Cogné-Laage, J.-F. Allemand, L. Jullien and A. Lemarchand, *J. Am. Chem. Soc.*, 2005, **127**, 15491–15505.

[15] A. Lemarchand and B. Nowakowski, *EPL*, 2011, **94**, 48004.

[16] P. Dziekan, L. Signon, B. Nowakowski and A. Lemarchand, *J. Chem. Phys.*, 2013, **139**, 114107.

[17] L. Signon, B. Nowakowski and A. Lemarchand, *Phys. Rev. E*, 2016, **93**, 042402.

[18] G. Morgado, B. Nowakowski and A. Lemarchand, *Phys. Rev. E*, 2018, **98**, 032213.

[19] D. T. Gillespie, *J. Chem. Phys.*, 2000, **113**, 297–306.

[20] C. Bianca and A. Lemarchand, *J. Chem. Phys.*, 2014, **140**, 224105.

[21] C. Bianca and A. Lemarchand, *J. Chem. Phys.*, 2014, **141**, 144102.

[22] C. Bianca and A. Lemarchand, *Physica A*, 2015, **438**, 1–16.

[23] D. T. Gillespie, *J. Chem. Phys.*, 1977, **81**, 2340–2361.

[24] J. Schnakenberg, *J. Theor. Biol.*, 1979, **81**, 389–400.

[25] P. Gray and S. K. Scott, *Chem. Eng. Sci.*, 1984, **39**, 1087–1097.

[26] J. D. Murray, *Mathematical Biology, I. An Introduction* (Springer, New York, 2002).

[27] G. B. Cook, P. Gray, D. G. Knapp and S. K. Scott, *J. Phys. Chem.*, 1989, **93**, 2749–2755.

[28] N. Fenichel, *J. Diff. Eq.*, 1979, **31**, 53–98.

[29] S. J. Fraser, *J. Chem. Phys.*, 1988, **88**, 4732–4738.

[30] C.W. Gardiner, *Handbook of Stochastic Methods for Physics, Chemistry and the Natural Sciences*, Springer, Berlin, 1985.

[31] G. E. Briggs and J. B. S. Haldane, *Biochem. J.*, 1925, **19**, 338–339.